1. Sherrif O. SAKA, 2. Saliu Ojo SEIDU, 3. S.A. TAIWO, 4. Iulian RIPOSAN

CHILLING EFFECT OF IRON POWDER ON THE MICROSTRUCTURE AND HARDNESS PROPERTY OF STRONGLY HYPEREUTECTIC GREY CAST IRON

1-3. Department of Metallurgical and Materials Engineering, Federal University of Technology, Akure, NIGERIA
4. POLITEHNICA University of Bucharest, ROMANIA

Abstract: In this work, the effects of iron (Fe) powder on strongly hypereutectic grey cast iron were experimentally verified. An in-stream inoculation technique was employed by producing grey cast irons. Chill wedges castings of type W, specified in the ASTM A367 of two different cooling moduli (CM) 0.11 cm and 0.35 cm (W_1 and W_3) were poured in sand mould at varied Fe-powder addition with constant FeSi–based inoculant (AlZr, Ca-FeSi alloy). The castings solidified within the strongly hypereutectic range with carbon equivalent (CE) at 4.60 and 4.89 %. The chill parameters were measured and evaluated. The double treated (0.2wt% Fe powder +0.3wt% FeSi and 0.4wt% Fe powder +0.3wt% FeSi) were observed to have given the optimum iron powder addition with best intermediate chilling result for W_1 while the single treated iron (0.3wt% FeSi) gave the best inoculating effect in general, in terms of the lowest carbides formation sensitiveness. The hardness tests showed that as the iron powder addition rate increased at double treatments, the hardness value increased consistently in thin section casting (W_1) with negative effect on graphite morphology of (0.6wt% Fe-powder + 0.3wt% FeSi) iron. The microstructures reveal uniformly distributed and randomly oriented graphite flakes in a pearlitic matrix particularly at slower rate of cooling (grey zones) with beneficial effect on the hardness property. The matrix structure of single treated iron for W_1 corresponds with W_3 of double treated iron at 0.2wt% Fe-powder.
Keywords: chilling, iron powder, hypereutectic grey iron, microstructure, hardness

1. INTRODUCTION

Grey cast iron is one of the most common and important material used in a wide range of application. Typical applications of grey cast iron are also in the automobile industries, manufacturing, pump impellers, base or beds of machineries. Grey cast iron being an oldest material, still remain a major cast material in many casting industries (approximately 45% of the world foundry industry production) (Figure 1), and as a result, an important material due to the outstanding properties such as heat conductivity, damping capacity, machinability etc. Besides, grey cast iron is easy to cast and is the most economical choice [1].
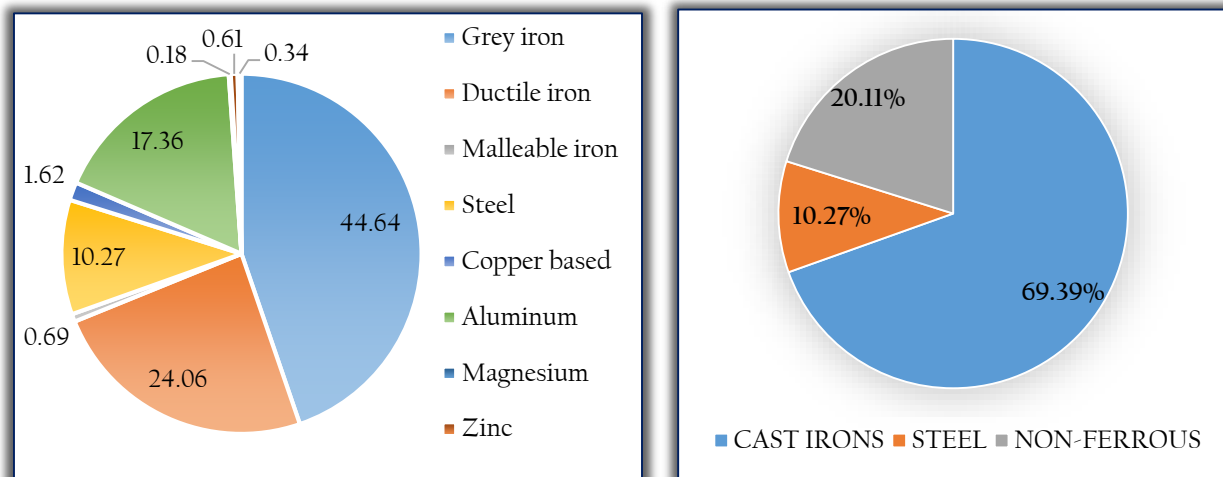

Figure 1: 2018 World foundry industry production [Modern Casting, Dec. 2017]

The basic material of grey cast iron consists of ferrous metal and graphite flakes. The size and the shape of the graphite flakes and the exact type of metal depend on the casting process [2]. The modifications of chemical composition, iron treatment and solidification pattern of grey cast iron have always been taken as a means of improving the properties of grey cast irons which invariably influence their performance in service. Due to the wide usage of grey cast iron, a lot of research has been done in this area to improve on its properties. These factors somewhat influence the chilling tendency (i.e. transition of stable graphite to metastable cementite) of cast iron depending on the sensitivity of casting sections. Among other factors that are particularly relevant to chilling behaviour during solidification (primary and eutectic solidification) are the relative nucleation and growth rate of graphite and cementite [1,3]. It is well known that the chilling tendency and graphite morphology in cast iron are basically controlled by inoculation, which acts on the formation and characteristics of the nuclei for graphite, and on the eutectic structure [4,5].

A lot of ongoing research on grey cast iron is increasing due to some defects experienced during casting. Among these defects are gas porosity, shrinkage porosity, and penetration problems which deteriorate the quality, and influence the grey cast iron production [6]. In another work, this type of defect was studied and characterized. It was found that this type of defect seems to be located around the primary austenite crystals, or dendrites, suggesting that the primary solidification and how its solidification structure is developed become important [7]. In previous works, iron powder has been used as an inoculant for the primary solidification as it has been considered to be the most effective nucleating particle for primary austenite dendrites due to the fact that its crystallographic structure is the same as the primary phase of the solidifying metal and also owing to the fact that the pure iron powder does not melt [8-10]. However, known research work available in this area has been established using iron powder and FeSi alloy to improve the chilling control in hypereutectic grey cast iron which also helps in the refinement of the grains [9,10]. Iron powder additions favour austenite dendrite formation in hypereutectic irons, acting as reinforcement for eutectic cells, but led to unsuitable substrate morphologies for graphite nuclei and consequently a lower eutectic cell count, especially at low cooling rates [10].

Apart from the use of pure iron powder which is inadequately available due to material and/or cost constraints, hence iron powder regarded as waste from local foundry and/or machine workshops can be recycled and profoundly used for various foundry additives. Therefore, the need to control the chilling tendency by inoculation (FeSi alloy inoculant) and promote primary solidification by iron powder addition can be achieved. This study therefore investigated the effect of iron powder additions with conventional inoculants on strongly hypereutectic grey cast irons which will invariably have a significant effect on the microstructure and hardness property of the grey cast iron that will meet the desired results for automobile industries. However, in this work, the chill wedge is applied in accordance to the traditional method of determining the tendency of a melt to solidify grey, mottle and white.

2. MATERIALS AND METHOD
⎯ Materials
The materials used for this research are scrap auto engine block, graphite, ferrosilicon (FeSi) based alloy/inoculants (CAS Pty Ltd), Limestone and iron powder (Fe – powder)

⎯ Production of Grey Cast Iron
The scrap auto engine block was broken down into smaller sizes that could enter through the opening of the furnace and was heated in a 40 kg graphite crucible furnace. The crucible pot was first preheated for about 15 mins to remove any form of moisture remained in the pot. After the first preheating, the crucible was placed in the furnace and preheated for the second time to a certain temperature before charging. Prior to the first melt, the ladles were preheated simultaneously by placing them on the lined cover in order to limit the heat loss.

The scraps of 20 kg were first charged through the opening of the crucible and subsequently 15 kg was charged during melting to make a total melt weight of 35 kg. During this course, 0.5 kg furnace FeSi foundry alloy, and then followed by 0.5 kg graphite were added. The crucible furnace was superheated to temperature of about 1,520° C, and at this temperature, the charges had become melted completely and ready for tapping. Iron powder and FeSi based alloy inoculant (74.22% Si, 1.21% Al, 1.21% Zr, 2.44% Ca, bal Fe) of particle sizes in the range 0.3 – 0.7 mm was added to the metal stream when tapping from the crucible to preheated ladle at 1,490°C temperature and poured at 1450° C. No iron powder was added to the first melt tapped which served as the initial cast iron for control sample. The second, third and fourth melts tapped were inoculated with varying addition of iron powder (0.2 wt.%, 0.4 wt.% and 0.6 wt.%) and constant addition of FeSi alloy 0.3wt% by weight of melt (6 kg) respectively. The addition began first with iron powder when the ladle was one-third full and was completed FeSi alloy when the ladle was two-third full. The first melt was inoculated or treated with FeSi inoculant only (single treated) while the subsequent melts were double treated (iron powder plus FeSi inoculant).

Standard chill wedges of W_1 [B=5.1mm, H = 25.4mm) and W_3, [B = 19.1mm, H = 38.1mm] specified in the ASTM A367-wedge test were explored [11] for this present experiment. After pouring the melt into the prepared green sand moulds, the castings were left for almost a day in the mould to avoid any hot shaking effects on the solid state transformation. The fettled cast chill wedge samples were fracture at the centre (midway of its length) in order to carry out macrostructure (fracture) analysis on the irons produced. The measurements of chills were obtained for each treatment by evaluating the following chill parameters: relative clear chill (RCC); relative mottled chill (RMC) and relative total chill (RTC) as shown in the equations 1 – 3 [12].

$$RCC \ = \ 100 \ (W_c \ / \ B) \ \% \qquad\qquad (1)$$
$$RTC \ = \ 100 \ (W_t \ / \ B) \ \% \qquad\qquad (2)$$
$$RMC = \ 100 \ (W_m \ / \ B) \ = \ 100 \ [0.5(W_t \ + \ W_c) \ / \ B] \ \% \qquad\qquad (3)$$

where, W_c is the clear chill zone of the wedge (portion nearest the apex, entirely free of any grey spots); W_m is the mottled zone (portion starting with the end of the clear chill and continuing to the last spot of visible cementite or white iron); W_t is the total chill zone (from the junction of the gray fracture with the first appearance of chilled iron to the apex); and B is

the maximum width of the test wedge. Hence, the Figure 2 indicates the three different zones- grey, mottled and white iron zones marked as point 1, 2, 3.

⎯ Characterization and Testing

The metallography examinations were done on each wedge sample in such a manner that three different points were chosen. The samples were examined under a metallurgical microscope at a magnification of 200X for the different treatments, and the micrographs of the un-etched samples and etched samples with Nital (2 % nitric acid and 98 % ethanol) were also obtained.

The chemical composition of each samples of the wedges were analyze in each of the wedge samples for all the iron treatments. This was achieved with the use of chemical composition analyzer (spectrometer).
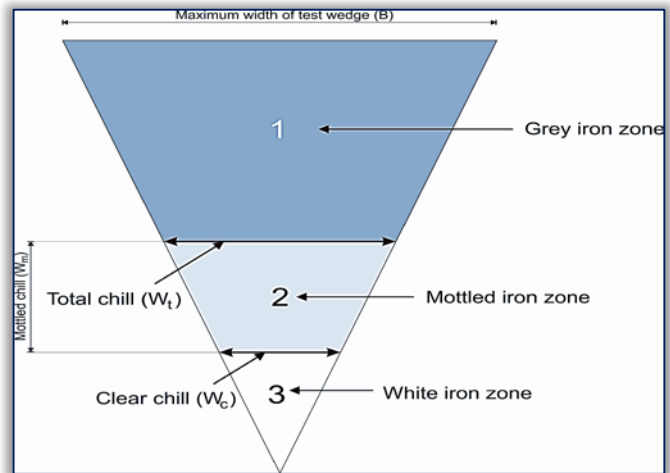

Figure 2: Grey iron (1), Mottled (2) and White (3) zones of the wedge sample and the dimensions representing W_t and W_c chill criteria

Hardness measurement was also performed on each wedge sample at three different points using the Rockwell hardness tester of type C (HRC) with a load of 150 kg. The average hardness values were estimated and recorded for each point on each of the wedge test sample.

3. RESULTS AND DISCUSSION

⎯ Chemical composition

The chemical analysis of the experimentally produced irons is shown in Table 1. The 3.61 - 4.04 %C, 2.45 - 2.91 %Si, 0.35 - 0.59 %Mn, 0.14 - 0.164 %S and 0.06 - 0.11 %P. Whereas, the typical residual elements were negligible because of their low levels. However, from the analysis, the evaluation of carbon equivalent (CE) proved that the produced cast irons fall within the hypereutectic cast irons. The result of this was traced to the addition of the local iron powder and likewise the inoculants added (inoculation treatment).

Table 1: Chemical Composition of Produced Irons

IRONS	CHEMICAL COMPOSITION, WEIGHT %						Carbon Equivalent C.E*	Mn/S	Mn x S
	C	Si	Mn	P	S	Al			
0.3wt% FeSi	3.61	2.91	0.59	0.067	0.146	0.0073	4.60	4.04	0.086
0.2wt%Fe- powder+ 0.3wt% FeSi	3.99	2.49	0.359	0.111	0.164	0.0013	4.86	2.19	0.059
0.4wt%Fe- powder+ 0.3wt% FeSi	4.04	2.45	0.354	0.106	0.140	<0.001	4.89	2.53	0.050
0.6wt%Fe- powder+ 0.3wt% FeSi	3.97	1.86	0.370	0.121	0.173	0.014	4.63	2.14	0.064

*CE = %C + 0.3 (%Si + %P) − 0.03%Mn + 0.4%S

⎯ Macrostructure

Tables 2 and 3 and Figures 2 and 3 show the results obtained from the macrostructure of the fractured wedge samples for irons produced. For all irons produced, the double treated iron (0.6 wt.% Fe-powder +0.3 wt.% FeSi) was recorded to have high chilling tendency from W_1 to W_3 for all chill criteria. However, the single treated iron (0.3 wt.% FeSi) was observed to have shown minimum chill tendency despite the small addition rate and poor ladle treatment compared with the large addition rate of cheap ferrosilicon alloy and with the typical values [12-15]. Hence, the single treated iron at 0.3 wt.% FeSi shows a consistent trend in reducing the chill for all wedge samples from RCC through RMC up to RTC. This however indicates the efficiency of the inoculant, chemical composition and likewise the effect of the casting thickness.

Table 2: Macrostructure (Fracture) Analysis of Wedge (W_1) Sample

IRON TREATMENT	W_1: CHILL CRITERIA					
	W_c (mm)	W_m (mm)	W_t (mm)	RCC (%)	RMC (%)	RTC (%)
0.3wt% FeSi alloy	1.18	2.40	3.61	12.97	26.72	39.67
0.2wt% Fe powder +0.3wt% FeSi alloy	2.72	3.55	4.38	29.89	39.01	48.13
0.4wt% Fe powder +0.3wt% FeSi alloy	2.94	4.03	5.11	32.31	44.23	56.15
0.6wt% Fe powder +0.3wt% FeSi alloy	3.19	4.54	5.89	35.05	49.89	64.73

Table 3: Macrostructure (Fracture) Analysis of Wedge (W_3) Sample

IRON TREATMENT	W_3: CHILL CRITERIA					
	W_c (mm)	W_m (mm)	W_t (mm)	RCC (%)	RMC (%)	RTC (%)
0.3wt% FeSi alloy	1.42	4.21	7.00	6.20	18.39	30.57
0.2wt% Fe powder +0.3wt% FeSi alloy	1.53	4.78	8.00	6.68	20.81	34.93
0.4wt% Fe powder +0.3wt% FeSi alloy	1.71	5.86	9.83	7.46	25.20	42.93
0.6wt% Fe powder +0.3wt% FeSi alloy	4.38	9.25	14.12	19.13	40.40	61.66

Generally, the chilling tendency decreases with increasing cooling modulus or casting thickness for W_1 and W_3 wedge samples for all iron treatments with variations for which they differ especially at the chilling evaluation parameters and some other prevailing factors. This was as a result of cooling rate, that is W_1- CM= 0.11cm at a fast rate of cooling and W_3- CM= 0.35cm (medium cooling rate) or as the cooling modulus values increases the chill tendency decreases [12]. Meanwhile, the difference between the single treated iron and the double treated irons varies in respect of the chill criteria, the cooling modulus (i.e. between the wedge samples) and the inoculation treatments effect (Figure 3).
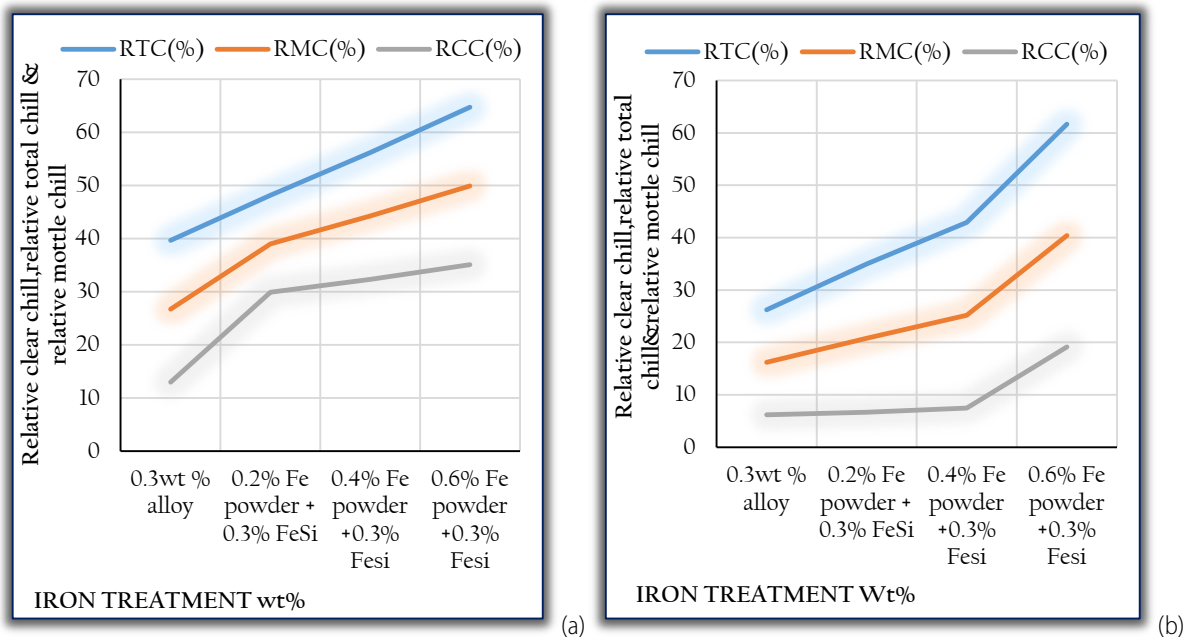
Figure 3: Influence of inoculation variant on chill criteria (RCC, RMC, RTC) for W_1 (a) and W_3 (b) wedge castings

For W_1 wedge sample, the difference between the single treated iron and the double treated irons (0.2wt% Fe-powder+ 0.3wt% FeSi and 0.4wt% Fe-powder+ 0.3wt% FeSi) decreases, but the difference between the single treated iron and the double treated iron (0.6wt% Fe-powder+ 0.3wt% FeSi) for W_1 and W_3 wedge samples increases (i.e. from RCC through RMC up to RTC). Similarly, the difference increases at both double treated irons (0.2wt% Fe-powder+ 0.3wt% FeSi and 0.4wt% Fe-powder+ 0.3wt% FeSi) for W_3. These differences at all double treated irons led to a high chill tendency most especially with RTC (35.05%) for 0.6wt% Fe-powder and RCC (16.92%) for 0.2wt% Fe-powder+ 0.3wt% FeSi; 19.34% for 0.4wt% Fe-powder+ 0.3wt% FeSi. This was due to fast solidification rate at highest cooling rate (W_1 wedge sample) and the effect of iron powder as it leads to high chill tendency [9,10].

In Figure 4, the single FeSi-based inoculant treated iron for W_1 wedge sample (highest cooling rate) resulted into a relative clear chill RCC comparable to double treated W_3 wedge (medium cooling rate) solidified irons, while the mottled and total chill evaluation of single treated iron for W_1 wedge sample is also comparable to double treated W_3 wedge irons. However, the difference in comparison between W_1-W_3 of double treated irons decreases in relation with chill evaluation criteria (i.e. RCC is larger than as RMC and RTC) except for the single treated iron in which the difference in comparison increases as RTC is larger than as RMC and RCC.

── Microstructure

For the single treated iron (0.3 wt.% FeSi Alloy addition), the micrograph of wedge test sample W1 (Table 4) shows that the chill zone consists of very fine, thin and close network of interdendritic graphite flakes accompanied in between by graphite inclusions and surrounded by cementite phase in a pearlitic matrix. The micrograph of the mottled zone revealed that the formation of TYPE-A graphite flakes has begun with more dispersed graphite inclusions observed while the grey

zone reveals further growth of very fine TYPE-A graphite flakes randomly oriented and uniformly distributed with few areas of TYPE-D interdendritic graphite in a pearlitic matrix. The presence of these inclusions were due to fast rate of solidification (rapid cooling rate), improper inoculants addition and somehow fading of inoculation treatment which cause the incomplete graphitization at eutectic solidification and euctectoid (solid state) transformation despite the fact that the chemistry of the single treated iron indicates high carbon and silicon content (Table 1) and also possesses aluminium content which is within the recommended range (0.005 - 0.01 %) [16, 17]. Also, the ratio of silicon to carbon Si/C ratio of the treated iron was 0.8 which correspond to the range (0.7 - 0.9) at which interdendritic graphite forms up at higher solidification rates [18]. More so, the MnS compounds possess less ability to nucleate graphite leading to Type-D graphite at higher cooling rate [19].

(a)

(b)

(c)
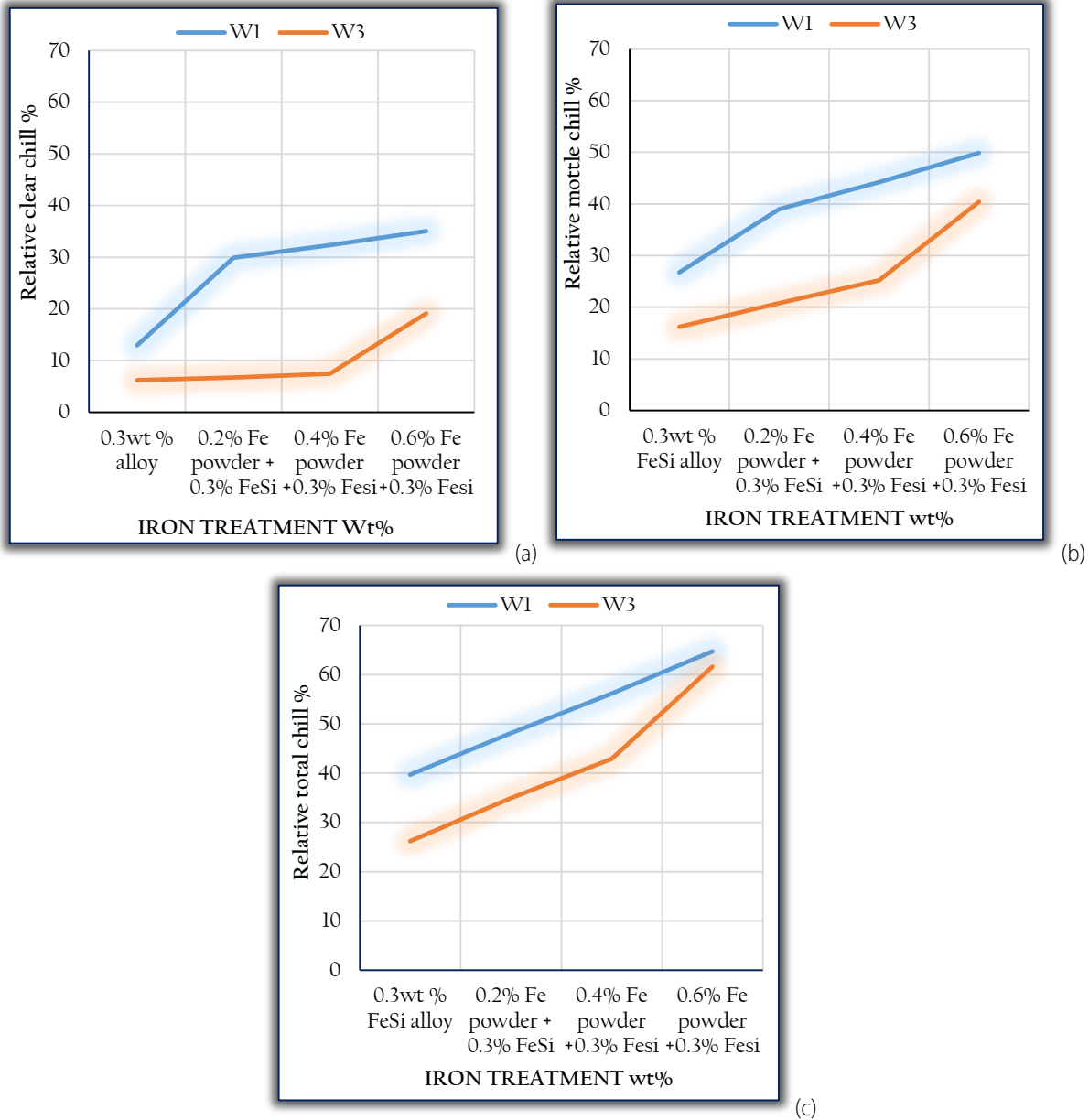
Figure 4: Comparison between W_1 and W_3 for RCC (a), RMC (b) and RTC (c) chill criteria

From Table 4, the microstructure of wedge test sample W3 where the chill zone revealed that there is a finer structure of Type-D interdendritic graphite flakes with very small areas of finer structure of Type -A graphite flakes with cementite phase in a pearlitic matrix. The small area of Type-A was due to the effect of inoculation despite the poor treatment and some other factors such as the %Mn × %S (0.086) which was above the recommended range (0.03 - 0.06) [19]. The mottled zone resulted to a morphology consisting of fine, thin and fairly uniform distribution and random orientation of Type-A graphite flakes. However, there are a little change in the morphology as the cooling proceeded to the grey zone which consists of more perfect randomly oriented and uniformly distributed Type-A graphite in a full fine pearlitic matrix due to the slow rate of cooling. The form and amount of this Type-A might be as a result of the incomplete secondary graphitization due to the improper MnS compound which serves as a major nucleation sites for graphite particularly at second stage of graphitization [20].

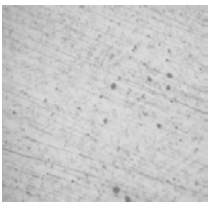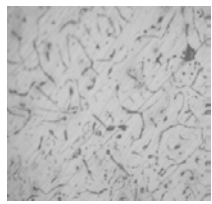Table 4: Microstructure/Graphite Morphology of Single Treated Iron (0.3wt% Fesi Alloy Addition) for W_1 and W_3 at X200
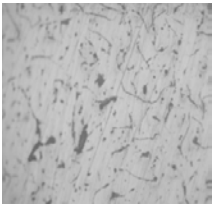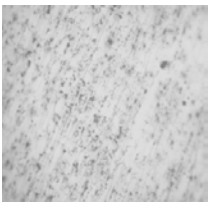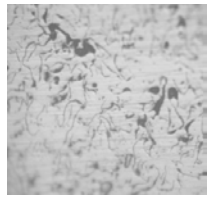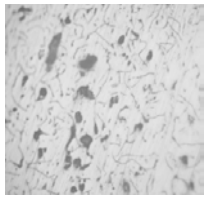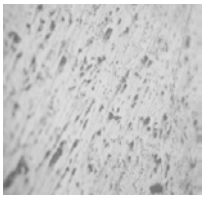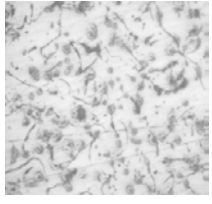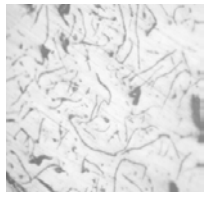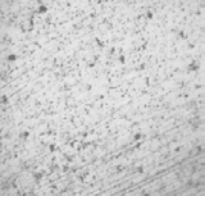
IRON TREATMENT	WEDGE SAMPLE	GREY ZONE	MOTTLE ZONE	CHILL ZONE
TREATED	W_1			
	W_3			

Table 5: Microstructure/Graphite Morphology of Double Treated Iron
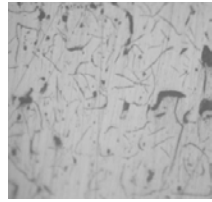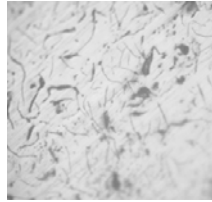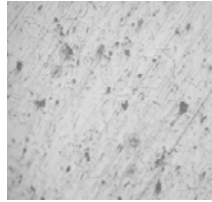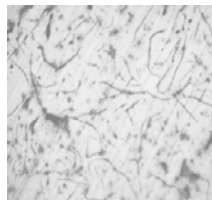(0.2wt% Fe-Powder + 0.3wt% FeSi Alloy addition) for W_1 and W_3 at X200
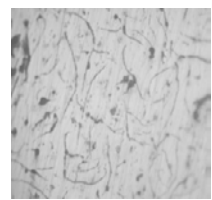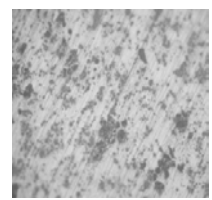
IRON TREATMENT	WEDGE SAMPLE	BASE POINT	MIDDLE POINT	TIP POINT
0.2wt%IRON POWDER+0.3wt% FeSi	W_1			
	W_3			

In Table 5, the micrographs show the microstructure morphology of 0.2wt% iron powder (Fe- Powder) + 0.3%wt FeSi alloy for wedge test sample W1 at various points. The chill zone consist of very five Type-D interdendritic graphite (undercooled graphite) surrounded by cementite phase in a pearlitic matrix because the fine flakes formed at larger degree of undercooling due to fast cooling and at this point the iron powder has less ability to nucleate graphite thereby leading to Type-D graphite due to the negative effect of Fe-Powder on MnS compound characteristics [21] despite the FeSi inoculants treatment after iron powder addition, high carbon equivalent (CE=4.86%), %Mn x %S (0.06) was found to be in the last section of recommended range. But the low level of residual aluminium (0.0013%Al) which is below the recommended range (0.005-0.010%Al) led to Type-D graphite as it affects the eutectic undercooling and recoalescence degree [16]. Meanwhile, the mottle zone (point 2) consisted of fine and thinner structure of Type-A graphite uniformly distributed and randomly oriented with slag inclusions in between the flakes surrounded by pealitic structure. The moderate cooling rate at this point shows that there was a decreased undercooling due to the addition of the inoculants (FeSi alloy). The high carbon and silicon content (CE=4.86%) also favoured the increase in graphitization potential which happen to be effective as a function of section sensitivity [20]. However, the high carbon and silicon content, proper %Mn x %S (0.051) which was within the range (0.03-0.06), proper inoculation treatments influence the formation of Type-A graphite despite low level of aluminium content. But the grey zone revealed imperfect or uneven distribution of Type-A graphite with random orientation in a pearlitic matrix with few traces of ferrite. Though the flakes are thicker still maintain the size compared to the mottle zone. This confirms the secondary graphitization occurrence.

Also in Table 5, the micrographs of W3 wedge test sample depict the microstructure morphology of treated (0.2wt% iron powder (Fe- Powder) + 0.3%wt FeSi alloy) iron with the chill zone showing very finer structure of Type-A graphite flakes uniformly distributed and randomly oriented alongside few areas of Type-D and some point graphites in a pearlitic matrix. This signifies the combine effect of the double treatment (Fe-Powder + FeSi Alloy) as the casting section thickness increases despite fast cooling rate. Whereas, the mottled zone consists of fairly uniform distributed and randomly oriented, thick and fine Type-A graphite flakes while microstructure of the grey zone observed on the micrograph shows a complete uniformly distributed and randomly oriented finer flakes of Type-A graphite in a full fine pearlitic matrix. This is as a result of high degree of nucleation [1] which is more pronounced at slow rate of solidification.
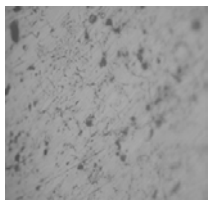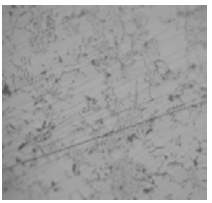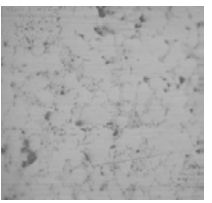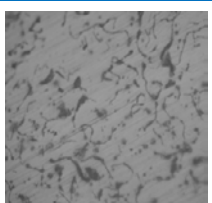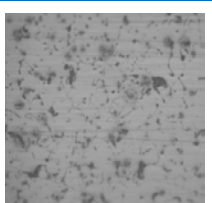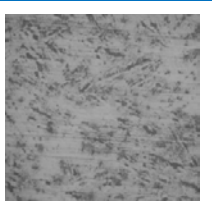
Table 6 refers to the micrographs of 0.4wt% iron powder (Fe- Powder) + 0.3%wt FeSi alloy treatment for W1 and W3 wedge test samples at three points respectively. The micrograph of W1 is pearlite. The chill zone of W1 showed very finer structure of Type-B rosette graphite and small areas of finer structure of Type-D interrdendritic graphite with graphite inclusions in between which might be due to high superheating, slow pouring rate, etc. The micrograph of the mottled zone (W1) showed randomly oriented but uneven distribution of very finer Type-A graphite. The Type-B disappeared as a result of increase in carbon content [1], which in turn increases the graphitization potential [22]. As a result of this more graphite formation is observed [10]. Likewise, the grey zone revealed Type-A graphite (uniformly distributed and randomly oriented). Occasionally, very small area of Type-C (kish graphite) was observed (a hypereutectic graphite form) due to the carbon equivalent (CE = 4.89%) but this point was able to form Type-A graphite due to effect of FeSi alloy treatment after iron powder addition. Despites slow pouring rate, extremely low aluminium content (< 0.0010) and proper %Mn x S% (0.05). Table 6 shows that the chill zone for W3 wedge sample was very fine Type-D graphite with inclusions in between whereas, the mottled zone revealed very few coarse flakes (Type-A) with uniform distribution and random orientation. This would have been as a result of formation of large austenite dendrites due to the effect of iron powder on primary austenite dendrites during eutectic liquid solidification and section thickness (related to cooling rate). While the grey zone showed more refined Type-A graphite flakes not coarse as those observed in the middle point, having random orientation and fairly uniform distribution. It was observed that on slow cooling rate, the graphite morphology tend to be a little more refined at the grey zone (a dependency on section thickness). Also, high carbon and silicon content influenced more graphite formation at this point. It was observed that the chill zones for W1 and W3 revealed Type-B or Type-D, and this could be due to the effect of iron powder addition (0.4wt%) especially in thin sections (high cooling rate) due to a limited graphitizing effect [23] despite the 0.3wt% FeSi treatment after the iron powder addition.

Table 6: Microstructure/Graphite Morphology of Double Treated Iron
(0.4wt% Fe-Powder + 0.3wt% FeSi Alloy addition) for W_1 and W_3 at X200

IRON TREATMENT	WEDGE SAMPLE	GREY ZONE	MOTTLE ZONE	CHILL ZONE
0.4wt%IRON POWDER+0.3wt% FeSi	W_1			
	W_3			

Generally, it was observed that from single treated iron (FeSi alloy treatment) to various double treated irons (iron powder addition + FeSi alloy treatment), the graphite amount increases as the cooling modulus increases and also graphite morphology tend to be more promoted and refined from large undercooling (undercooled graphites) to moderate undercooling (medium-sized Type-A graphite) more especially at the grey and mottled zones of single treated (0.3wt.% FeSi alloy) and 0.2wt.% Fe-powder + 0.3wt.% FeSi alloy.

Table 7: Microstructure/Graphite Morphology of Double Treated Iron
(0.6wt% Fe-Powder + 0.3wt% FeSi Alloy addition) for W1, and W3 at X200

IRON TREATMENT	WEDGE SAMPLE	BASE POINT	MIDDLE POINT	TIP POINT
0.6wt%IRON POWDER+ 0.3wt% FeSi	W_1			
	W_3			

The micrographs (Table 7) showing the graphite morphology of 0.6wt.% + 0.3wt.% FeSi alloy for W1 revealed at all points finer structure of Type-D graphite where the size and branch network increased. The iron powder effect (0.6wt% Fe-Powder) showed undesirable morphology from chill zone (high cooling rate), up to mottle zone (moderate cooling rate) and grey zone (slow cooling rate) with no effect of 0.3wt% FeSi alloy treatment after the iron powder addition.

The W3 wedge sample for 0.6wt% Fe-Powder + 0.3wt% FeSi alloy showed that the micrograph of the chill zone consists of imperfect finer structure of Type-E interdendritic graphite surrounded by cementite phase in a pearlitic matrix whereas the mottle zone consists of Type-A graphite which has begun to form with random orientation and fairly even distribution with few areas of cementite and pearlite. Also, small trace Type-E graphite remained and likewise the grey zone but with increase in graphite size in a full pealitic matrix.

Obviously, increase in the addition rate of iron powder with fixed amount of FeSi alloy treatment after iron powder addition affect the graphite morphology mostly pronounced at 0.6wt% iron powder addition + 0.3wt% FeSi alloy treatment followed by 0.4wt% iron powder addition + 0.3wt% FeSi alloy treatment, and with little or no effect at 0.2wt% iron powder addition + 0.3wt% FeSi alloy treatment more especially at the tip point (chill zone) of all wedge test samples (W1 and W3). However, this correlate with the chill parameters evaluated and slightly with the chemical composition of each iron produced despite the differing melt conditions. Also, the effect of cooling rate, chemical composition, differing thermal characteristics of sand mould, and section thickness on the wedge samples (i.e. from thin sections-W1 to medium section-W3) were highly observed. The thickness of the flakes observed most especially at 0.2wt% iron powder addition + 0.3wt% FeSi alloy treatment was due to nearly 100% complete graphitization and likewise the quality of the graphite flakes was majorly due to the effect of the alloy treatment added.

— Hardness

The various hardness tests at three points (zones) on each wedge sample (W_1 and W_3) were carried out and the average values for each zone were determined (Table 8).

As shown in Figure 5, the average hardness value for the three wedge samples at each zones. The average hardness values decrease with addition of 0.3wt% FeSi alloy (single treated iron) but increase were recorded in hardness values of double treated irons with varied addition of iron powder [(0.2wt%,0.4wt%,0.6wt%) + FeSi alloy]. However, the decrease in hardness was as a result of the inoculation treatment as the high silicon content increases the cementite instability [24].

Table 8: Hardness Value (HRc) of Wedge Sample W_1 and W_3

WEDGE SAMPLE	IRON TREATMENT	AVERAGE HARDNESS VALUE (HR_C)			TOTAL AVERAGE HARDNESS VALUE (HR_C)
		GREY ZONE	MOTTLE ZONE	CHILL ZONE	
W_1	0.3wt% FeSi	21.50	22.40	23.40	22.30
	0.2wt%Fe-Powder+0.3wt% FeSi	21.50	25.70	28.90	25.40
	0.4wt%Fe-Powder+0.3wt% FeSi	27.50	29.60	36.70	31.26
	0.6wt%Fe-Powder+0.3wt% FeSi	29.70	35.40	39.60	34.90
W_3	0.3wt% FeSi	21.30	18.80	24.30	21.50
	0.2wt%Fe-Powder+0.3wt% FeSi	17.70	22.90	21.20	20.60
	0.4wt%Fe-Powder+0.3wt% FeSi	19.20	24.00	25.30	22.80
	0.6wt%Fe-Powder+0.3wt% FeSi	31.00	37.10	45.00	37.70

For the single treated iron, the chill zone (Figure 5a) of the wedge samples (W_1 and W_3) showed the highest hardness value with W_3 higher than W_1. The reason for this was due to the mould/metal interface and it might be from the inoculating effect as regard section sensitivity in relation to the mould/metal contact of each of the wedge samples. Also, the mottle zone of the wedge sample W_1 recorded higher hardness value than W_3 (Figure 5b). While the grey zone (Figure 5c) differs by recording a decrease in hardness from W_1 to W_3. However, the differences in the average hardness value (Figure 5) were observed to be very minimal and this indicates the degree of effectiveness of inoculation treatment despite poor inoculation.

The addition of constant rate of 0.3wt% FeSi alloy after iron powder addition at various rate (0.2wt%, 0.4wt%, 0.6wt %) hardness tests result. In this case of double treatments (iron powder + FeSi alloy), there is an appreciable and consistent trend in the way the hardness values increase as the iron powder addition rate increase. The tip (chill zone) of each of the wedge test sample for 0.2wt%, 0.4wt%, 0.6wt% Fe-Powder + (0.3wt% FeSi alloy) recorded the highest hardness value with 0.6wt% Fe-Powder showing highest hardness value (W_1-39.6HRC; W_3-45.0HRC) followed by 0.4wt% Fe-Powder (W_1-36.7HRC; W_3-25.3HRC) and 0.2wt% Fe-Powder (W_1-28.9HRC; W_3-21.2HRC). The hardness value recorded at the tip of all wedge test samples corroborate with chilling parameters evaluated and the microstructure analysed. Similarly, the mottle and grey zones concurred with 0.2wt% ranging from 25.7HRC to 22.9HRC and 21.5HRC to 17.7HRC. Likewise, the mottle and grey zones of 0.4wt% followed the same trend; 27.5HRC to 19.2HRC and 29.6HRC to 24.0HRC (i.e. ranges from W_1 to W_3 in a decreasing manner). While the mottle and grey zones of 0.6wt% range from 35.4HRC to 37.1HRC and 29.7HRC to 31.0HRC with W_3 wedge sample recording the highest hardness value at both zones in an increasing manner (Figure 5a

and 5b). Meanwhile the difference experienced in the average hardness value (Table 8) at each zone on the wedge test samples for 0.6wt% Fe-Powder + 0.3wt% FeSi alloy treatment correlates with the chill parameters evaluated and microstructure analyzed.
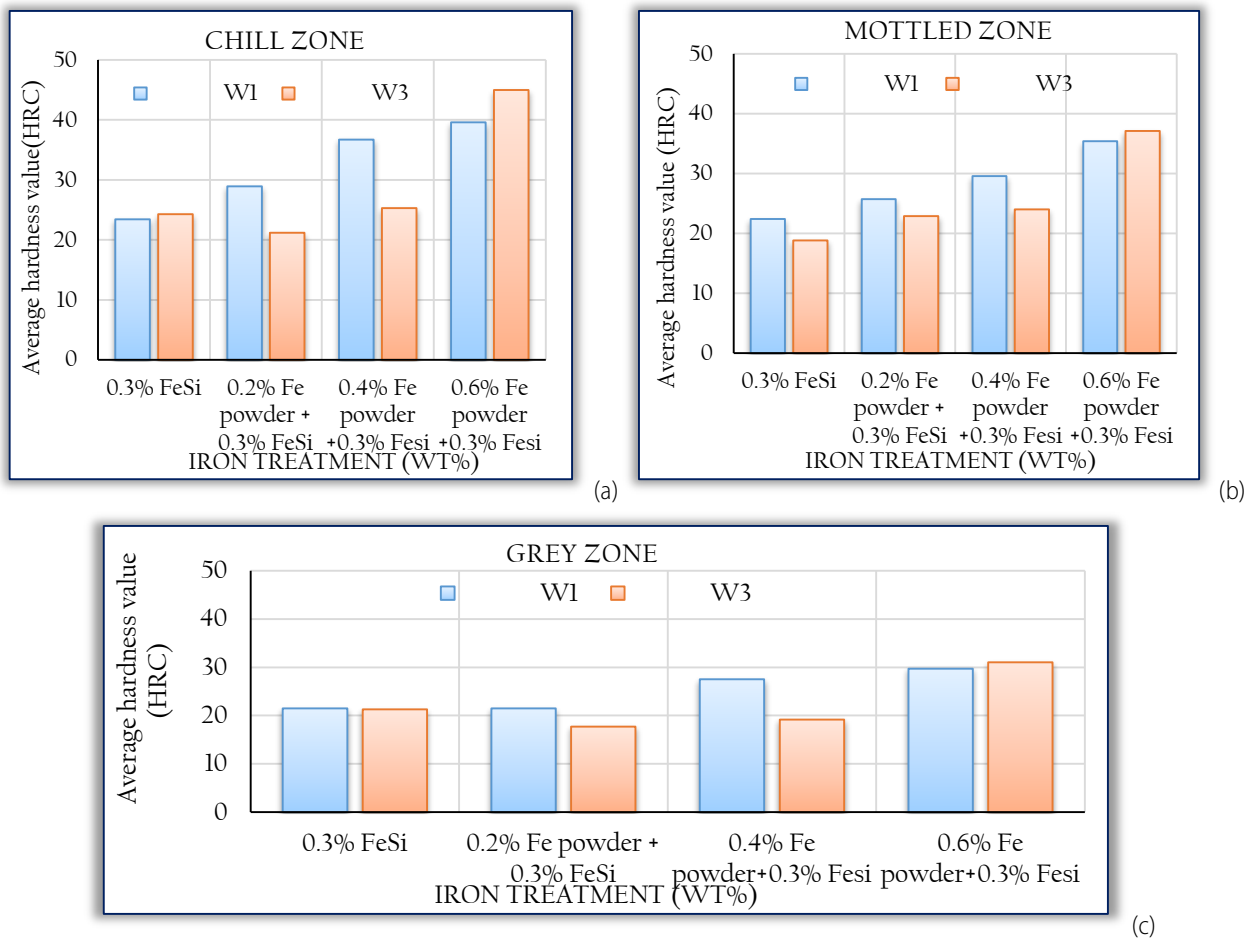

(a)

(b)

(c)

Figure 5: Average hardness values of various iron treatments of W_1 and W_3 wedge castings:
a) chill zone; b) mottled zone; c) grey zone

It could also be observed (Figure 5) that, the hardness values for thin section casting W_1 increase despite a constant inoculation treatment after iron powder addition while the medium section casting recorded a decrease in hardness values from single treated iron (0.3wt% FeSi alloy) to double treated (0.2wt% Fe-Powder addition + 0.3wt% FeSi alloy treatment) iron. If the wedge test sample W_3 could experience this, hence, the $W_{3\frac{1}{2}}$ and W_4 [ASTM A 367] would therefore show more decrease in the hardness value as the iron powder addition rate increases.

4. CONCLUSIONS

At the end of this research, the following conclusions were drawn;

⎯ the study showed that as the iron powder addition rate increases, the chill tendency increases slightly relative to addition rate with increase in hardness;

⎯ the higher the amount of carbon, the more the graphite formation;

⎯ it was also shown that from single treated iron (FeSi-based inoculant addition) to various double treated irons (iron powder addition + FeSi alloy treatment) the graphite amount increases as the cooling modulus increases. Graphite morphology also tend to be more promoted and refined from large undercooling (undercooled graphite) to moderate undercooling (medium-sized Type-A graphite) more especially at the grey and mottle zones of single treated (0.3wt.% FeSi alloy) and 0.2wt.% Fe-powder + 0.3wt.% FeSi alloy.

⎯ the grey cast iron produced revealed varying size of graphite flakes which are randomly oriented in pearlitic matrix, more pronounced at moderate and slow cooling rates;

⎯ the chemistry of the casts plays a major role in chill reduction and modification of graphite flakes particularly for the single treated iron while double treated irons, despite high carbon equivalent (CE=4.6−4.89%), the effect Mn and S contents with varied residual aluminium lead to relatively high chill, especially at the high cooling rates (thin section casting) for 0.6wt% Fe powder + 0.3wt% FeSi alloy;

⎯ the double treated irons (0.2wt% Fe powder + 0.3wt% FeSi alloy and 0.4wt% Fe powder + 0.3wt% FeSi alloy) proved to have given the optimum iron powder addition;

—— the double treatments resulted into intermediate chill and medium-sized Type A graphite with more desirable performance obtained by inoculation treatment (0.3wt% FeSi) after iron powder addition at 0.2wt% and 0.4wt% Fe-powder. The Ferrosilicon addition was able to control the chill tendency favourably especially at 0.2wt% Fe-powder.

References

[1]   Singh, V. (2009): Physical Metallurgy. Standard Publishers Distribution, 1705 Nai Sarak, New Delhi-110006. Pp. 446-463.
[2]   Hong Jiang, Yiyong Tan, Junfery Lei (2003): Auto analysis system for graphite morphology of gray cast iron", Journal of automated methods of management in chemistry, Vol.25, No. 4, pp. 87-92.
[3]   Elmquist, L., Adolfsson, S. and Diószegi, A. (2008): Characterizing shrinkage porosity in gray cast iron using microstructure investigation', AFS Trans. 116, pp. 691 – 703.
[4]   Riposan, I., Chisamera, M., Stan, S., Toboc P., Ecob C., white D., (2008):   Al,Zr-FeSi Preconditioning of Grey Cast Iron", Material Science and Technology, Vol. 24 (5), pp 578-584.
[5]   Elkem AS Foundry Products Division, (2012): Cast Iron Inoculation- The Technology of Graphite Shape Control, ISO 9001.
[6]   Ruff, G. F. and Wallace, J. F. (1977): effect of solidification structures on the tensile properties of grey iron AFS Trans.85, pp.179-202.
[7]   Glover, D., Bates, C. E. and Monroe, R. (1982): The relationships among carbon equivalent, micro-structure and solidification characteristics and their effects on strength and chill in gray cast iron AFS Trans. 90: pp. 745-757.
[8]   Riposan, I., Chisamera, M., Stan, S. and Barstow, M. (2012): Improving Chill Control in Iron Powder Treated Slightly Hypereutectic Grey Cast Iron, China Foundry, Vol. 8, No. 2, pp. 228-229.
[9]   Chisamera M., Riposan I., Stan S., and Barstow M. (2011): Structure Characteristics of Iron Powder Treated Slightly Hypereutectic Grey Irons, Int. J. Cast. Metals. Res., 2011, 24(6), pp 370–377.
[10]   Riposan, I., Chisamera, M., Stan, S. and Barstow, M. (2011): Influence of Iron   Powder Addition on the Solidification and Structure of Slightly Hypereutectic Gray Cast Iron, AFS Trans., 119, p 389–406.
[11]   American Society for Testing of Material, ASTM Standard A367-60, 2005: Standard Test Methods of Chill Testing of Cast Iron. West Conshohocken: ASTM; p. 2.
[12]   Stan, S., Chisamera, M., Riposan, I., Stefan, E., and Barstow, M.(2010): Solidification Pattern of Un-inoculated and Inoculated Gray Cast Irons in Wedge Test Samples. Transactions of the American Foundry Association (AFS), Vol. 118, pp 295-309.
[13]   Seidu S.O. and Ogunniyi I. O. (2012): Control of Chilling Tendency in Grey Cast Iron Reuse. Material Research vol.16 no.1 São Carlos Jan./Feb. 2013 Epub Nov 22, 2012 ISSN 1516-1439.
[14]   Seidu S.O. (2009): Inoculants effect on chilling tendency in Ductile Iron. In: Proceedings of the International PhD Foundry Conference; 2009; Brno. Brno University of Technology.
[15]   Riposan I, Chisamera M, Stan S and White D. (2007): Chilling properties of Ba/Ca/Sr inoculated grey cast irons. International Journal of Cast Metals Research, 20(2), pp 90-97.
[16]   Riposan, I., Chisamera, M., Stan, S., Hartung, C. and White, D. (2010): Three-Stage Model for the Nucleation of Graphite in Grey Cast Iron, Material Science Technology 26(12), pp. 1439–1447.
[17]   Chisamera, M., Riposan, I., Stan, I. and Skaland, T. (2004): Investigation of Effect of Residual Aluminium on Solidification Characteristics of Un-Inoculated and Ca/Sr Inoculated Gray Irons. AFS Transactions, vol.107, Paper 04-096.
[18]   Bockus, S. (2006): A Study of the Microstructure and Mechanical Properties of Continuously Cast Iron Products. METABK 45 (4) pp. 287-290.
[19]   Gundlack, R. (2008): Observations of Structure Control to Improve the Properties of Cast Irons. The 2008 Honorary Cast Iron Lecture, Div. 5, AFS Metalcasting Congress, Atlanta, Paper 08-158.
[20]   Taşliçukur, Z., Altuǧ, G., Polat, Ş., Hakan, Ş., Atapek, and Türedi, E. (2012): Characterization of Microstructure and Fracture Behavior of GG20 and GG25 Cast Iron Materials used in Valves Brno, Czech Republic, EU.
[21]   Stan S, Chisamera M, Riposan I, Ivan N, Barstow M. Iron Powder Treated Gray Irons - Critical Shape Characteristics for Graphite Nuclei. Journal of Materials Engineering and Performances, 2012, 21 (8): 1793-1799.
[22]   Chisamera, M., Riposan, I., Stan, I. and Skaland, T. (2004): Investigation of Effect of Residual Aluminium on Solidification Characteristics of Un-Inoculated and Ca/Sr Inoculated Gray Irons. AFS Transactions, vol.107, Paper 04-096.
[23]   Stefanescu, D. M. (1989): Classification and Basic Metallurgy of Cast Iron, Metals Handbook, Vol. 1, 10th Ed. ASM International, Materials Park Ohio, USA. Pp. 4-7.
[24]   Higgins, R.A. (2004): Engineering Metallurgy: Applied Physical Metallurgy, 6th ed. viva books, New Delhi, pp. 355-356.